Direct Observation of the Single-Domain Limit of Fe Nanomagnets by Spin-Polarized Scanning Tunneling Spectroscopy

A. Yamasaki,[1,2] W. Wulfhekel,[2] R. Hertel,[2] S. Suga,[1] and J. Kirschner[2]
[1]*Graduate School of Engineering Science, Osaka University, Osaka 560-8531, Japan*
[2]*Max-Planck Institut für Mikrostrukturphysik, Weinberg 2, 06120 Halle, Germany*
(Received 23 March 2003; published 16 September 2003)

We have investigated the magnetic structure of self-organized Fe islands on W(001) by means of spin-polarized scanning tunneling spectroscopy (Sp-STS). Single-domain, simple vortex, and distorted vortex states have been observed. The high resolution magnetic images were used to experimentally determine the single-domain limit. The experimental structures were compared with results of micromagnetic calculations confirming the ground state nature of the experimental configurations. The single-domain limit directly observed with Sp-STS is consistent with theoretical predictions.

DOI: 10.1103/PhysRevLett.91.127201 PACS numbers: 75.75.+a, 07.79.Cz, 75.70.Rf

The magnetic properties of nanoscale magnets are of high importance in magnetics and magnetoelectronics. Studying the magnetism of nanoscale magnets is not only beneficial for the progress of general magnetism but is also important for the development of high-density magnetic storage devices and magnetic random-access memory [1–4]. The question of the single-domain limit in information storage is of practical importance. To ensure reliable read-write processes, the particle should be a magnetically bistable system. The corresponding magnetic configurations are typically single-domain states with mutually opposite magnetization direction. Formation of magnetic domains is, generally speaking, technologically undesirable. In soft-magnetic nanoscale particles, micromagnetic calculations predict that various stable or metastable magnetic states exist, e.g., single domain, vortex, flower, *C* state, or others [5–10]. The formation of these various magnetic states originates from the competition between the stray field energy and the exchange interaction. In small particles, the exchange interaction dominates and the structure is mostly homogeneous, i.e., single domain, whereas in larger particles the tendency to reduce the stray field dominates and flux-closure patterns are formed. Although the phase diagram of magnetic states in nanometer thick elements has been studied from the theoretical approach and a consistent picture for the single-domain limit has been established [6,8,9,11,12], no direct experimental evidence has been reported yet. In order to investigate the magnetic states in nanoscale structures, indirect measurements [13] and different magnetic microscopy, e.g., magnetic force microscopy (MFM) as well as transmission electron microscopy [14,15], have been employed. With MFM, the vortex state was studied intensively [16–18]. However, no direct observation of the single-domain limit was feasible due to the limited lateral resolution of the imaging techniques.

Recently, the vortex core in Fe islands on W(110) has been resolved using spin-polarized scanning tunneling spectroscopy (Sp-STS) [19]. Sp-STS offers the necessary lateral resolution to fully resolve the details of the magnetization state. As Stroscio *et al.* mentioned [20], spin-dependent contrast in scanning tunneling spectroscopy (STS) may be acquired by using a spin-polarized surface state [21–24]. Because of the essential difference between the contrast mechanisms of MFM and Sp-STS, Sp-STS offers a superior spatial resolution (potentially down to atomic scale) to MFM as has been shown experimentally [25] and theoretically [26]. In this Letter, we present the first direct study on the single domain to vortex state transition using high resolution Sp-STS. We further compare our experimental results with micromagnetic calculations.

The single-domain limit of small ferromagnetic particles is a frequently addressed concept [27] although there are numerous possible definitions, depending on whether energetic [28], dynamic [29], or stability considerations [10,11] are made. Our investigation relies on a definition based on stability, since one may observe experimentally any stable domain structure. Information about the energy of the arrangement is not available from the experiment. It may, however, be obtained via micromagnetic simulations.

The experiments were performed in an ultrahigh vacuum chamber system for sample and tip preparation and characterization as well as cryogenic scanning tunneling microscope (STM). For scanning, we used chemically etched polycrystalline W tips and followed the method of Bode [21]. After flashing the tip to ≈ 2200 K, we deposited ≈ 10 ML Fe onto the tip followed by annealing. As has been reported [23], these tips have an in-plane magnetization. The magnetic nanostructures were prepared by deposition of 4.7–6.5 ML of Fe on W(001), followed by annealing to ≈ 800 K. This results in the formation of magnetic nanostructures [30,31]. The surface cleanliness of substrate and film were confirmed by Auger electron spectroscopy and low-energy electron diffraction. During magnetic imaging, the sample was cooled to ≈ 30 K. Magnetic contrast was obtained with tunneling

spectroscopy using a lock-in technique. In this technique, differences in the density of states of minority and majority electrons lead to a spin-dependent differential conductance when measured with a spin-polarized tip [21]. From this, the relative orientation between tip and sample magnetization can be concluded. The presented magnetic images were obtained with a modulation voltage of 30 mV at a frequency of 6.7 kHz.

The observed magnetic domain pattern of the magnetic nanostructures was compared with micromagnetic simulations. The micromagnetic code is based on the finite element method combined with the boundary element method [32]. The finite element mesh consists of tetrahedral cells of irregular shapes, whose dimensions are below the exchange length $l_s = \sqrt{2\mu_0 A/J_s^2} \approx 3.7$ nm of Fe (J_s is the saturation magnetization). Within the elements, the magnetization profile was approximated by linear functions. The principle of the micromagnetic algorithm consists in minimizing the total energy as a function of the orientation of the magnetization at each discretization point. The energy terms involved are stray field, anisotropy, and exchange energy. For the calculation of the anisotropy energy, the cubic magnetocrystalline anisotropy of Fe is considered up to the second nonvanishing order. The stray field energy is calculated by introducing a scalar potential U from which the stray field is derived as a gradient field $H = -\nabla U$. The potential U is the solution of Poisson's equation. A more detailed description of the code is given in Ref. [33]. A powerful feature of the finite element method is its geometrical versatility which allows one to model magnetic structures in particles of any shape. This enables us to directly compare the experimental results with micromagnetic simulations on an island of the same shape. In order to account for magnetization states which might be unexpected, we let the program find the structures by starting from random configurations, rather than assuming an initial configuration close to an expected structure.

In order to acquire spin-sensitive dI/dU images, we chose the spin-polarized surface state of Fe(001) [20]. For this, STS spectra of an Fe whisker with well-defined Fe(001) single crystal surfaces have been recorded [see Fig. 1(a)]. The spectra were measured near the left and right edges of the long axis of the Fe whisker corresponding to the areas of opposite magnetization due to the flux closure in the whisker. The peak of the surface state in both spectra is seen at the same energy $U = 0.13$ V [20,34,35]. The intensities of the peaks, however, differ significantly. This difference is due to spin-dependent tunneling since (i) the peak originates from the d-like surface state of minority spin [20], and (ii) the relative orientation of magnetization is reversed going from one to the other side of the whisker. We used the same surface state in the Fe nanostructures. A topographic image of self-organized Fe islands measured by means of STM with normal W tip is shown in Fig. 1(b). Several Fe islands

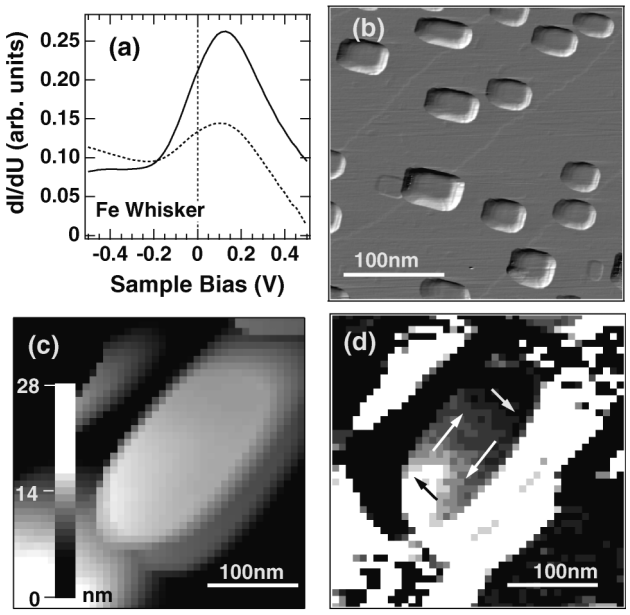

FIG. 1. (a) STS spectra for an Fe whisker. Solid and dotted lines show spectra with parallel and antiparallel orientation between the in-plane component of the magnetization of the tip and the magnetization of the whisker, respectively. (b) Topographic image of low coverage Fe islands on W(001). The image is differentiated to make the edge of the islands clearer. The differentiation leads to an illumination of the islands from the bottom right. (c) Topographic image of an Fe island on W(001) at $U = 0.20$ V. (d) Magnetic dI/dU image of the same Fe island with a magnetic vortex state on W(001) at $U = 0.20$ V. The arrows illustrate the orientation of the magnetization.

can be seen on a pseudomorphic 2 ML Fe film. The sizes and thicknesses are around 50 and 8 nm, respectively. The size of the Fe island can be controlled by changing the amount of deposited Fe and varying the annealing temperature. The several nm thick Fe islands have the lattice constant of bulk Fe [31]. At these thicknesses, the islands show the same electronic structure as bulk Fe on the surface. Maps of the differential conductivity were taken at an applied voltage of 0.15 or 0.20 V, i.e., close to the peak maximum of the surface state. The pseudomorphic Fe double layer which is present between the Fe nanostructures, has a totally different density of states [36].

Figures 1(c) and 1(d) show the topographic and magnetic dI/dU images of an elliptic Fe island on W(001) measured by Sp-STS with Fe coated W tip. The major and the minor axis and the height of the island are about 200, 100, and 11 nm, respectively. The island has an atomically flat top. The contrast in the dI/dU image reflects the in-plane magnetization of the sample. The magnetic configuration of the island in Fig. 1(d) is a vortex as concluded from the bright, dark, and intermediate areas that can be clearly seen in Fig. 1(d). The dI/dU image of the vortex is similar to images reported previously [19]. The arrows represent the orientations of magnetization in each area of

the vortex. The sense of rotation of the vortex, however, is unknown since the absolute orientation of the tip magnetization is not known. From the observation, we cannot conclude whether the vortex state in this island is metastable or the ground state. For larger islands of similar thickness, we always found the vortex state and never a single-domain state, indicating that the vortex state is the ground state. Note that the edge of the islands in the dI/dU images shows a strong black (white) contrast due to rapid shrinking (extending) of the piezo during scanning across the edges. The contrast is not of magnetic origin but is due to the above-mentioned extrinsic effect. Further, one may observe a contrast in island-free areas that is due to the thin pseudomorphic carpet of Fe covering the W(001) surface. This contrast is not of magnetic origin but is due to the totally different density of states in few ML thin pseudomorphic Fe films. For the magnetic interpretation of the islands, we restrict ourselves to well-defined islands with atomically flat surfaces that have a homogeneous electronic structure.

Smaller islands, such as those displayed in Figs. 2(a) and 2(b), never showed a vortex state but always a homogenous contrast. These two images of Figs. 2(a) and 2(b) were obtained in the same scan, i.e., the tip conditions are the same. The dI/dU signal of the two Fe islands is remarkably different, indicating a different direction of magnetization. Therefore, we can conclude that the magnetization of one island is nearly antiparallel to that of the other island and both islands are in the single-domain state. Note that in the islands a weak bright (or dark) area can be seen close to some edges. According to recent calculations, the magnetic moments close to the edge slightly curl their orientations from the average magnetization direction in the island to reduce the stray field (so-called "onion" state) [10]. This is consistent with the images of the single-domain islands.

We have observed other magnetic structures in larger Fe islands as shown, e.g., in Fig. 3(a). The magnetic dI/dU image has large bright and dark areas. The relative position of the areas appears, however, different from that of a vortex state at first glance [see Fig. 1(d)]. This deviation from the vortex state of ideally round disks is caused by the irregular island's shape. In order to interpret the dI/dU contrast in the image, we have calculated the magnetic structure of this irregular island with micromagnetic simulations. In our case, a finite element mesh has been generated according to the topological image of the Fe island to allow direct comparison of the experimental and simulated domain pattern. According to the simulations, there are two possible candidates of magnetic stable or metastable states, i.e., single domain and vortex state. However, the single-domain state yields not only a higher total energy but also a much different dI/dU image compared to the experimental one. The calculated vortex state is shown in Fig. 3(b). Although the contrast close to the vortex core in the calculation is not found in the experiment, the calculated contrast agrees well with the experimental one. Obviously, the vortex core is not imaged with full resolution, possibly due to a weak magnetostatic interaction between the tip and the sample [24]. The observed magnetic state is in qualitative agreement with the calculations, predicting that the vortex state, not the single-domain state, is the ground state.

From the magnetization pattern of many islands observed with Sp-STM, the experimental magnetic phase diagram shown in Fig. 4 was obtained. The single-domain state was always found below a thickness of 6 nm and an average diameter of 120 nm. The average diameter of the island is defined as $(a + b)/2$, if the island has an elliptic shape with a and b as the two axes. The directly observed experimental boundary between the single-domain and vortex states is well reproduced by analytical and numerical calculations by Cowburn *et al.* [13] and others [10]. In the self-organized nanostructures, we observed aspect ratios up to 2. For these aspect ratios, calculations show no shift of the single-domain limit [11]. For more elliptical particles,

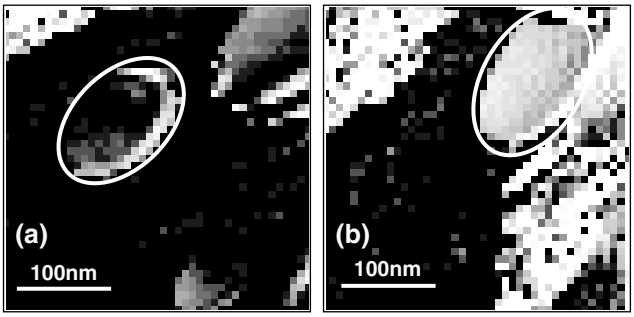

FIG. 2. Magnetic dI/dU images of Fe islands with magnetic single-domain (onion) states on W(001) at $U = 0.20$ V. (a) and (b) show the Fe islands (marked by ellipses) which have the different orientations of the magnetization.

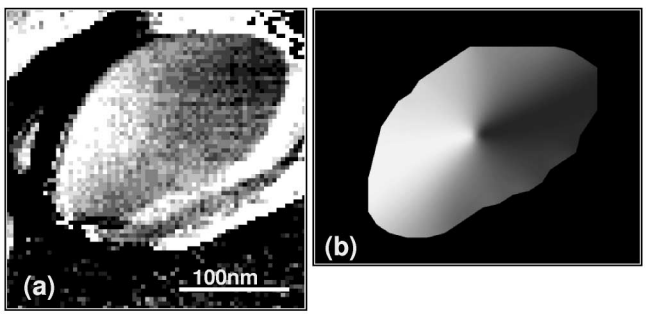

FIG. 3. (a) Magnetic dI/dU image of an Fe island with modified vortex state on W(001) at $U = 0.15$ V. (b) Calculated vortex state for irregular Fe island. About 35 500 elements were used in the micromagnetic simulation.

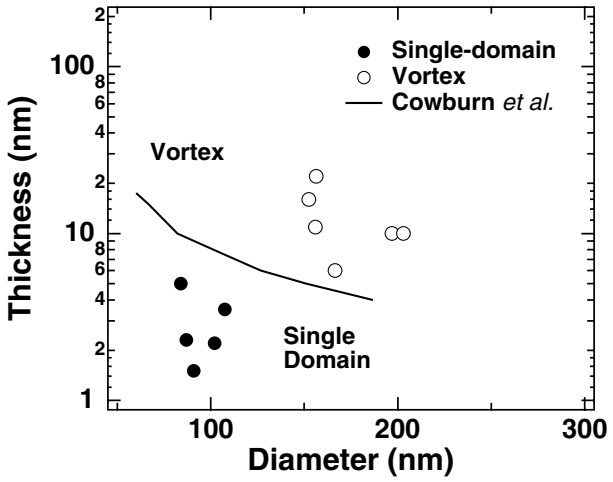

FIG. 4. A phase diagram of the magnetic states for different diameters and thicknesses of the Fe islands on W(001). Solid and open circles show the single-domain and vortex state, respectively. The solid line is the dividing line following calculations by Cowburn *et al.* [13].

however, the single-domain limit is slightly shifted towards smaller islands as numerical simulations indicated [11].

In conclusion, we present in-plane magnetic images of single-domain and vortex states of self-organized Fe nanostructures on W(001) by means of spin-polarized scanning tunneling spectroscopy with Fe coated W tips. The experimentally found single-domain limit is well reproduced by previous theoretical calculations. We further compared observed and calculated distorted vortex states in irregular islands. The single-domain limit of elliptical islands with aspect ratio below 2 obtained experimentally is consistent with the results of calculations by Cowburn *et al.* and by Ha *et al.* for circular islands, indicating a weak dependence on the shape.

The authors thank J. K. Ha for fruitful discussions.

[1] J.-G. Zhu, Y. Zheng, and G. A. Prinz, J. Appl. Phys. **87**, 6668 (2000).
[2] C. Stamm, F. Marty, A. Vaterlaus, V. Weich, S. Egger, U. Maier, U. Ramsperger, H. Fuhrmann, and D. Pescia, Science **282**, 449 (1998).
[3] K. J. Kirk, J. N. Chapman, and C. D. W. Wilkinson, Appl. Phys. Lett. **71**, 539 (1997).
[4] K. Bussmann, G. A. Prinz, S.-F. Cheng, and D. Wang, Appl. Phys. Lett. **75**, 2476 (1999).
[5] Y. Zheng and J.-G. Zhu, J. Appl. Phys. **81**, 5471 (1997).
[6] W. Rave and A. Hubert, IEEE Trans. Magn. **36**, 3886 (2000).
[7] H. Kronmüller and R. Hertel, J. Magn. Magn. Mater. **215–216**, 11 (2000).
[8] N. A. Usov, L. G. Kurkina, and J. W. Tucker, J. Phys. D **35**, 2081 (2002).
[9] R. Hertel, Z. Metallkd. **93**, 957 (2002).
[10] J. K. Ha, R. Hertel, and J. Kirschner, Phys. Rev. B **67**, 064418 (2003).
[11] N. A. Usov, C.-R. Chang, and Z.-H. Wei, J. Appl. Phys. **89**, 7591 (2001).
[12] W. Rave, K. Fabian, and A. Hubert, J. Magn. Magn. Mater. **190**, 332 (1998).
[13] R. P. Cowburn, D. K. Koltsov, A O. Adeyeye, and M. E. Welland, Phys. Rev. Lett. **83**, 1042 (1999).
[14] R. D. Gomez, T. V. Luu, A. O. Pak, K. J. Kirk, and J. N. Chapman, J. Appl. Phys. **85**, 6163 (1999).
[15] M. Schneider, H. Hoffmann, S. Otto, Th. Haug, and J. Zweck, J. Appl. Phys. **92**, 1466 (2002).
[16] T. Shinjo, T. Okuno, R. Hassdorf, K. Shigeto, and T. Ono, Science **289**, 930 (2000).
[17] J. Raabe, R. Pulwey, R. Sattler, T. Schweinböck, J. Zweck, and D. Weiss, J. Appl. Phys. **88**, 4437 (2000).
[18] S. P. Li, D. Peyrade, M. Natali, A. Lebib, Y. Chen, U. Ebels, L. D. Buda, and K. Ounadjela, Phys. Rev. Lett. **86**, 1102 (2001).
[19] A. Wachowiak, J. Wiebe, M. Bode, O. Pietzsch, M. Morgenstern, and R. Wiesendanger, Science **298**, 577 (2002).
[20] J. A. Stroscio, D. T. Pierce, A. Davies, R. J. Celotta, and M. Weinert, Phys. Rev. Lett. **75**, 2960 (1995).
[21] M. Bode, M. Getzlaff, and R. Wiesendanger, Phys. Rev. Lett. **81**, 4256 (1998).
[22] O. Pietzsch, A. Kubetzka, M. Bode, and R. Wiesendanger, Phys. Rev. Lett. **84**, 5212 (2000).
[23] M. Pratzer, H. J. Elmers, M. Bode, O. Pietzsch, A. Kubetzka, and R. Wiesendanger, Phys. Rev. Lett. **87**, 127201 (2001).
[24] A. Kubetzka, M. Bode, O. Pietzsch, and R. Wiesendanger, Phys. Rev. Lett. **88**, 057201 (2002).
[25] S. Heinze, M. Bode, A. Kubetzka, O. Pietzsch, X. Nie, S. Blügel, and R. Wiesendanger, Science **288**, 1805 (2000).
[26] D. Wortmann, S. Heinze, Ph. Kurz, G. Bihlmayer, and S. Blügel, Phys. Rev. Lett. **86**, 4132 (2001).
[27] A. Aharoni, IEEE Trans. Magn. **27**, 4775 (1991).
[28] R. Hertel and H. Kronmüller, J. Magn. Magn. Mater. **238**, 185 (2002).
[29] E. H. Frei, S. Shtrikman, and D. Treves, Phys. Rev. **106**, 446 (1957).
[30] E. Bauer, Appl. Surf. Sci. **11–12**, 479 (1982).
[31] W. Wulfhekel, F. Zavaliche, F. Porrati, H. P. Oepen, and J. Kirschner, Europhys. Lett. **49**, 651 (2000).
[32] D. R. Fredkin and T. R. Koeler, IEEE Trans. Magn. **26**, 415 (1990).
[33] R. Hertel, J. Appl. Phys. **90**, 5752 (2001).
[34] W. A. Hofer, J. Redinger, A. Biedermann, and P. Varga, Surf. Sci. **466**, L795 (2000).
[35] T. Kawagoe, E. Tamura, Y. Suzuki, and K. Koike, Phys. Rev. B **65**, 024406 (2001).
[36] S. Bodea, W. Wulfhekel, and J. Kirschner (unpublished).